Catal Lett (2009) 130:169–176
DOI 10.1007/s10562-009-9844-y

# Template Preparation of Highly Active and Selective Cu–Cr Catalysts with High Surface Area for Glycerol Hydrogenolysis

**Changhai Liang · Zhiqiang Ma · Ling Ding · Jieshan Qiu**

Received: 21 November 2008 / Accepted: 5 January 2009 / Published online: 17 January 2009


**Abstract** High surface area Cu–Cr catalysts had been prepared via a facile carbon template route, and characterized by $N_2$ physisorption, temperature-programmed reduction, X-ray diffraction, Raman spectroscopy, and transmission electron microscopy. The catalytic properties of the nanostructured Cu–Cr catalysts were evaluated by glycerol hydrogenolysis. The results show that the specific surface area of the obtained Cu–Cr catalyst can reach above 50 $m^2$/g, while those of CuO and $Cr_2O_3$ are about 10 and 50 $m^2$/g, respectively. The surface areas of Cu–Cr catalysts can be controlled by carbon template, Cu/Cr molar ratio, and treatment atmosphere and final temperature. The reduced Cu–Cr catalysts show significant catalytic activity and selectivity in glycerol hydrogenolysis, i.e. above 51% conversion of glycerol and above 96% selectivity to 1,2-propanediol in 4.15 MPa $H_2$ at 210 °C. The Cu–Cr catalysts with low Cu/Cr molar ratio present high conversion of glycerol, which is different from the conventional copper-chromite catalyst.

**Keywords** Glycerol · Hydrogenolysis · Cu–Cr catalyst · Carbon template · High surface area

## 1 Introduction

Biodiesel derived from vegetable oil and animal fat has emerged as a viable fuel [1]. About 1 kg crude glycerol would be formed as by-product when 9 kg biodiesel was produced. Therefore, converting glycerol to value-added chemicals has attracted, therefore, great interest from both a fundamental and an applied point of view. Several catalytic conversion processes had been reported to glycerol into useful chemicals by means of oxidation, hydrogenolysis, dehydration, esterification, carboxylation and gasification [2–14]. Among those routes, selective hydrogenolysis of glycerol to propylene glycol is a promising route to increase the profitability of biodiesel plant. Propylene glycol is an important chemical in polyester resins, liquid detergents, pharmaceuticals, functional fluids cosmetics, flavors and fragrances [15]. At present, propylene glycol is industrially produced mainly by using non-renewable sources, i.e. propylene oxide derived from propylene.

At the presence of metalllic catalysts and hydrogen, glycerol can be transformed into 1,2-propanediol and/or 1,3-propanediol, depending on the different pathways of hydrogenolysis as shown in Scheme 1 [5]. The use of diluting glycerol at high temperatures under high pressures is high energy consumption and limits its industrial application. Although lots of advances in glycerol to propylene glycol have been made within the past few years, the selectivity is still low. Recently low pressure hydrogenolysis of a concentrated glycerol solution to propylene glycol had been developed by Suppes' group [15]. A commercial copper-chromite was identified as the most effective catalyst. After reduced in $H_2$ at 300 °C for 4 h, the catalyst gave an 85% selectivity to 1,2-propanediol with a 55% glycerol conversion under moderate reaction conditions in a specially designed multi-clave reactor.

Conventional copper-chromite catalysts were prepared by a modified Adkins route [16], and the specific surface area of the obtained catalysts is low, only about 30 $m^2$/g.

C. Liang (✉) · Z. Ma · L. Ding · J. Qiu
Carbon Research Laboratory, State Key Lab of Fine Chemicals, School of Chemical Engineering, Dalian University of Technology, 158 Zhongshan Road, P.O. Box 49, 116012 Dalian, People's Republic of China
e-mail: changhai@dlut.edu.cn

**Scheme 1** Reaction pathways of glycerol hydrogenolysis

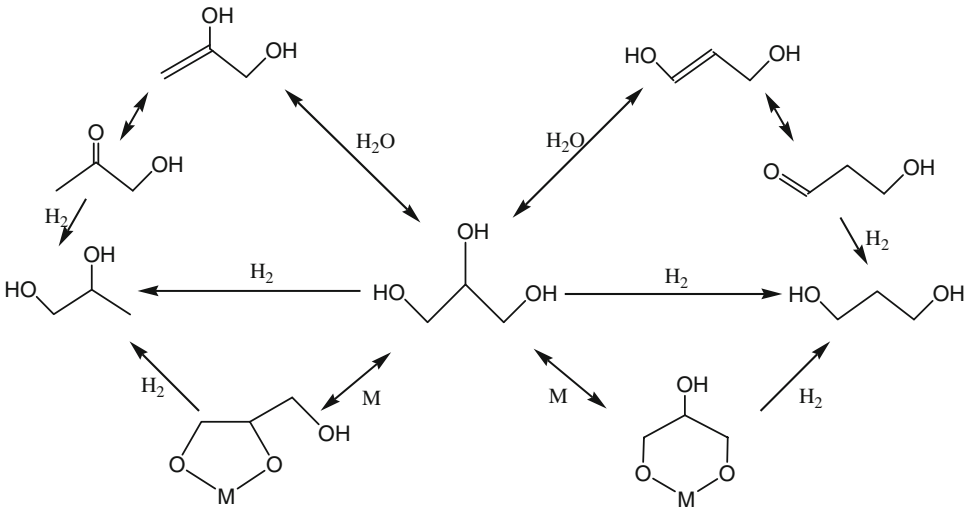


Therefore, it is necessary to find a new route to prepare high surface area copper-chromite catalysts. The recently reported carbon template method has been shown to be successful for synthesis of zeolite, metals, and oxides with high surface area [17–24]. The method allowed an effective control of the particle size of the resulting materials by adjusting the conditions of synthesis. For example, Schwickardi et al. had reported that $Cr_2O_3$ with a BET surface area of 156 $m^2/g$ can be obtained by an activated carbon route [18]. Our group had successfully prepared high surface area $CeO_2$, $ZrO_2$, $Fe_2O_3$, $Zr_xCe_{1-x}O_2$, and $Zr_xFe_{1-x}O_2$ using ultrahigh surface area carbon material as template [19, 24]. To the best of our knowledge, high surface area copper-chromites have not been reported by using carbon template route although other methods have been tried to synthesize high surface area samples [25–27]. In this work, we firstly demonstrate that the carbon template route allows synthesizing high-surface area Cu–Cr catalysts, which show high activity and selectivity to 1,2-propanediol in glycerol hydrogenolysis.

## 2 Experimental

### 2.1 Preparation of Cu–Cr Catalysts

All chemicals are used as received without further purification. Activated carbon and carbon aerogel were used as carbon templates in this study. The activated carbon is prepared by a direct chemical activation in which petroleum coke is reacted with excess KOH at 900 °C to produce the carbon materials containing potassium salts. These salts are removed by successive water washings [19]. The surface area of the carbon materials measured by Brunaure-Emmett-Teller (BET) method is about 3,234 $m^2/g$, the pore volume is about 1.78 $m^3/g$ and the average pore size is about 2.2 nm. Carbon aerogel was prepared by a microemulsion-templated sol–gel polymerization method [28]. The BET surface area, the pore volume and average pore size of the carbon aerogel are 661 $m^2/g$, 1.48 $cm^3/g$ and 7.1 nm, respectively.

Typically, about 3 g of the carbon materials were impregnated at room temperature with about 15 ml aqueous solution of copper nitrate and chromium nitrate mixture of different molar ratios for 30 min. Alternatively, impregnation was performed with a slight excess of solution. The slurry was then filtered and squeezed to remove the liquid on the carbon surface that could cause the formation of large oxide particles. After drying in air at 70 °C overnight, the resulting sample was transferred to a quartz reactor inside a tubular resistance furnace. The furnace was then ramped at 1 °C/min to final temperature and was held for 120 min. The atmosphere was in the presence of argon before 300 °C, and then shifted into a mixture gas of 20% $O_2$ in Ar at a flow rate of 120 ml/min. The conversion is almost 100% from copper nitrate and chromium nitrate to final copper and chromium oxide catalyst, and the ratio of Cu to Cr was obtained from the initial molar ratio of copper nitrate to chromium nitrate. After removal of the carbon template, the obtained oxides were stored for further characterization.

### 2.2 Characterization

TG/DTG experiments were also performed in Mettler Toledo TGA/SDTA851$^e$ thermogravimetry to understand decomposition process of copper nitrate and chromium nitrate and the removal temperature of carbon template. The samples were placed in the atmosphere of 80% Ar and 20% $O_2$ and heated at 5 °C/min to the final temperature of 750 °C.

Nitrogen adsorption and desorption isotherms with multi-point method at −196 °C were measured using Micromertics 2020. Prior to the measurements, all samples were degassed at a temperature of 300 °C at vacuum level of $10^{-3}$ Torr for at least 3 h. Surface areas were calculated from the linear part of the BET plot.

X-ray diffraction (XRD) analysis of the samples was carried out using a D/MAX-2400 diffractometer with Cu Kα monochromatized radiation source ($\lambda = 1.5418$ Å), operated at 40 kV and 100 mA. The average particle size of the samples was evaluated by the Scherrer formula from the half-width of the XRD peak corrected for instrumental broadening:

$$L = \frac{0.9\lambda_{K\alpha_1}}{B_{(2\theta)}\cos\theta_{\max}}$$

where $\lambda_{K\alpha_1}$ is 1.54178 Å, $B_{(2\theta)}$ is a full width at half-maximum of diffraction peak in radians.

Visible laser Raman spectra were recorded on Acton spectrograph (SpectraPro300i) coupled with a liquid nitrogen cooled CCD detector and the laser line at 532 nm was used as the excitation source.

The particle size and distribution of the samples were analyzed by transmission electron microscopy (JEM, 200 kV). Powder samples were ultrasonicated in ethanol and dispersed on holey carbon films on copper grids. Energy dispersive X-ray spectroscopy (EDX) was also performed in the same microscopy.

Temperature-programmed reduction (TPR) of the samples was carried out in a stream of 90% argon and 10% hydrogen with a flowing rate of 50 $cm^3$/min. The sample was heated at 10 °C/min from room temperature to 900 °C. The amount of the hydrogen consumption during the reduction was estimated with a thermal conductivity detector.

### 2.3 Activity Test

Glycerol hydrogenolysis was carried out in a 100 ml stainless steel autoclave in $H_2$ (4.15 MPa) at 210 °C for 600 min. About 70 ml aqueous solution of 40 wt% glycerol was used as the reactant. The catalyst used was 5% of glycerol in weight. After the reaction, the sample was cooled to room temperature and centrifuged at 9,000 r/min for 5 min to remove the catalyst. The products were analyzed with an Angilent 6890 gas chromatograph equipped with a flame ionization detector. ChemStation software was used to collect and analyze the data. A FFAP GC column (30 m × 0.32 mm × 0.5 μm) was used for separation. An *n*-butanol solution of a known amount of internal standard was prepared a priori and used for analysis. In order to compare with the conventional catalyst, a copper-chromite with Cu/Cr molar ratio of 1:1 was also evaluated under the same conditions. Prior to reaction, the catalyst was reduced by $H_2$ at 340 °C for 4 h.

## 3 Results and Discussion

Figure 1 shows TG/DTG curves of the activated carbon impregnated with copper nitrate and chromium nitrate in the atmosphere of 80% Ar and 20% $O_2$. As can be seen in Fig. 1a, mass loss of about 35% between 170 and 260 °C can be attributed to the decomposition of $Cu(NO_3)_2$ and the partial removal of carbon template. The maximum rate of mass loss occurs at 240 °C due to the formation of CuO besides a shoulder peak at about 190 °C which may be due to the formation of $Cu(NO_3)_2 \cdot 2Cu(OH)_2$. After the decomposition of $Cu(NO_3)_2$, there is still a mass loss, which could be attributed to combustion of the carbon. In the case of the $Cr(NO_3)_3$ impregnated activated carbon (Fig. 1b), the mass loss of about 19% between 100 and 200 °C can be attributed to the decomposition of $Cr(NO_3)_3$. In Fig. 1c, two peaks at 175 and 225 °C can be assigned to the decomposition of $Cr(NO_3)_3$ and $Cu(NO_3)_2$. The decomposition temperature of $Cr(NO_3)_3$ raised from 170 to 175 °C, while the decomposition temperature of $Cu(NO_3)_2$ moved to 225 °C, maybe due to formation of $CuCr_2O_4$. The maximum rate of mass loss occurs at 225 °C. Further mass loss is due to removal of carbon template. The carbon combustion is completed at temperature higher than 340 °C. As reported by Schwickardi et al. [18], metal nitrate catalyzes the combustion of the carbon template. At the presence of transition metal nitrates, the catalytic effect is even more obvious, indicating a combined effect of the nitrate and metal ions. The pronounced catalytic effect is caused by the presence of Cu, where an explosion takes place and the reaction is quite vigorous. Therefore, the $Cu(NO_3)_2$ impregnated activated carbon firstly was decomposed in the atmosphere of argon in our preparation, and then carbon template was removed by combustion in the 20% $O_2$ in Ar. The powders obtained afterward had a low surface area of about 13 $m^2$/g although the vigorous reaction can be avoided.

Table 1 provides a survey of the samples prepared by the carbon template route, including the textural parameters and phase composition. It was consistently observed that the carbon template route produced catalyst with surface areas substantially higher than those of samples by simply drying and calcination without carbon. Cu–Cr catalysts were prepared from two carbon materials: activated carbon and carbon aerogel. As can be seen, the type of carbon template has a substantial influence on the quality of the products. The sample of $Cr_2O_3$ prepared with the activated carbon after calcination at 500 °C had a surface area of 40 $m^2$/g, whereas that prepared with carbon aerogel

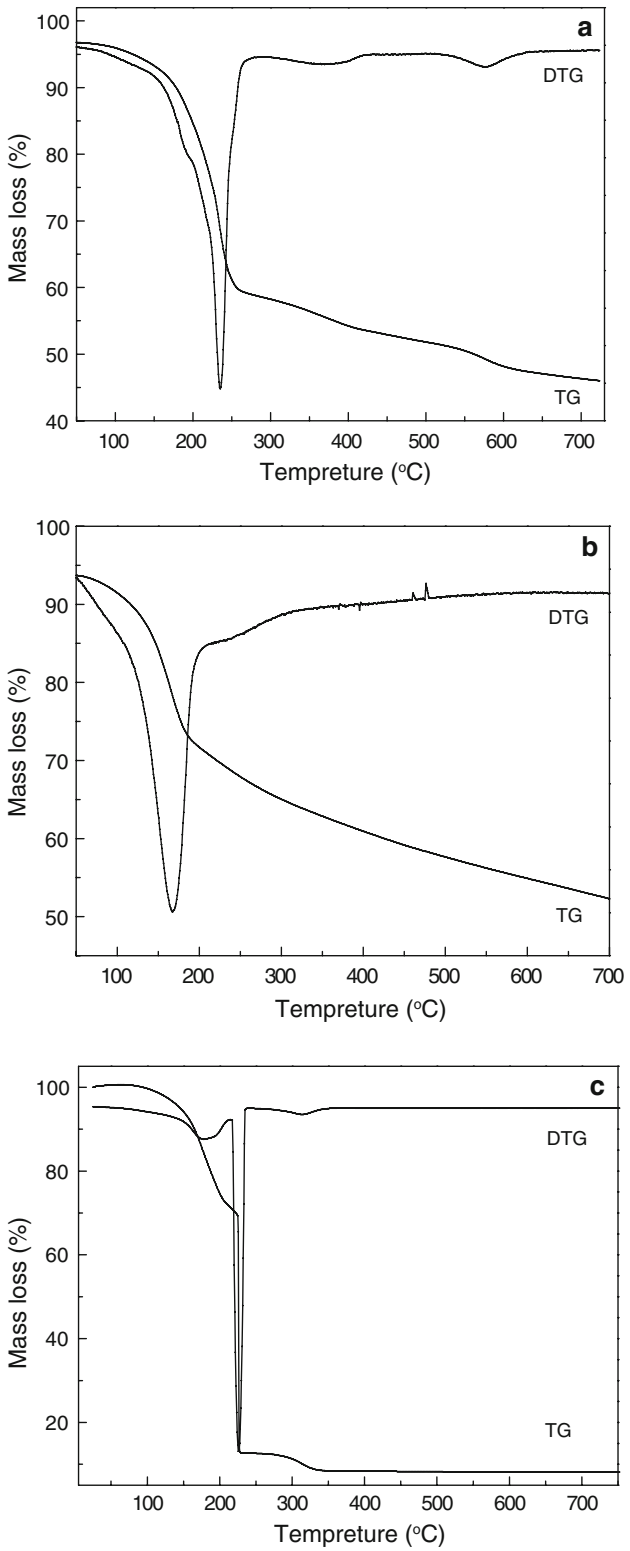


**Fig. 1** TG/DTG curves of the samples **a** $Cu(NO_3)_2$, **b** $Cr(NO_3)_3$, and **c** $Cu(NO_3)/Cr(NO_3)_3$ on the activated carbon

exhibited a surface area of about 87 $m^2/g$. For copper-chromite, the BET surface area can be as high as 177 $m^2/g$, however, this high value is not reproducible. When we tried to reproduce the sample, a surface area of only 55 $m^2/g$ was obtained. This could be due to the character of the templates used in the process. The above-mentioned results are similar to that reported by Schwickardi et al. [18]. The textural data are typically reproducible within 10% error. The two carbon materials gave high-surface-area Cu–Cr oxides although they have different pore structure and surface properties.

From Table 1, it was also found that Cu/Cr molar ratio has an important effect on the surface area of Cu–Cr oxides. The surface area of CuO is low by using either activated carbon or carbon aerogel as template. This is due to easy aggregation of CuO at high temperature. The same phenomenon also occurs in Cu–Cr oxides with high Cu loading. For instance, the surface areas of the samples with Cu/Cr molar ratios of 2:1 and 5:1 are 20 and 10 $m^2/g$, respectively. With the decrease of Cu/Cr molar ratio, the surface areas of the samples show the increasing trend. The surface areas of the samples with Cu/Cr molar ratios of 1:1 and 1:5 are 56 and 88 $m^2/g$, respectively. The sample with Cu/Cr molar ratios of 1:2 gave a middle surface area (33 $m^2/g$), which may be due to formation of $CuCr_2O_4$.

Preparation of metal oxides by the carbon template route is sensitive to the treatment atmosphere and the temperature programme used. As above-mentioned, Cu and Cr ions can catalyze the combustion of the carbon template before the oxide is completely formed. It is possible that formation of large particle due to sintering results in a rapid loss of the surface area under the conditions. The $Cr_2O_3$ samples by using carbon aerogel as template had a surface area of 40 $m^2/g$ at a final temperature of 500 °C. If oxygen concentration was limited in combusting process after 300 °C, the resulting $Cr_2O_3$ powder gave a surface area of above 65 $m^2/g$. To have an even more controlled combustion of the carbon template, argon was firstly passed over the sample for a time while the oven was being heated to 450 °C over 60 min, and then argon was changed to $O_2$/Ar mixture (1:5) and heated to 500 °C for a time. The $Cr_2O_3$ sample by this procedure gave a surface area of 87 $m^2/g$.

Figure 2 shows XRD patterns of CuO, $Cr_2O_3$ and Cu–Cr catalysts from activated carbon template. The crystalline phases were identified by comparing with ICDD files (CuO, 48-1548; $Cr_2O_3$, 38-1479; $CuCr_2O_4$, 26-0509). The characteristic peaks of CuO and $Cr_2O_3$ were clearly observed in the CuO and $Cr_2O_3$ samples. In the sample with Cu/Cr molar ratio of 1:5, the diffraction peaks due to $Cr_2O_3$ become wide, especially at about 35°. This could be due to the formation of $CuCr_2O_4$. When Cu/Cr molar ratio is 1:2, no peak due to $Cr_2O_3$ could be observed in the XRD pattern and the broad peak at about 35° can be identified as $CuCr_2O_4$. The average particle sizes of CuO, $Cr_2O_3$ and $CuCr_2O_4$ are about 35, 28, and 18 nm, respectively,

**Table 1** Phase composition and surface area of typical samples obtained by carbon template route

| Template | Precursor | Calcination(°C) | Phases composition | $S_{BET}$($m^2$ $g^{-1}$) |
|---|---|---|---|---|
| AC | $Cu(NO_3)_2$ | 500 | CuO | 13 |
| AC | $Cr(NO_3)_3$ | 500 | $Cr_2O_3$ | 40 |
| AC | $Cu(NO_3)_2/Cr(NO_3)_3 = 1:1$[a] | 500 | CuO, $CuCr_2O_4$ | 55 |
| AC | $Cu(NO_3)_2$ | 350 | CuO | <10 |
| AC | $Cr(NO_3)_3$ | 350 | $Cr_2O_3$ | 45 |
| AC | $Cu(NO_3)_2/Cr(NO_3)_3 = 1:1$[a] | 350 | CuO, $CuCr_2O_4$ | 56 |
| AC | $Cu(NO_3)_2/Cr(NO_3)_3 = 1:2$[a] | 350 | $CuCr_2O_4$ | 33 |
| AC | $Cu(NO_3)_2/Cr(NO_3)_3 = 2:1$[a] | 350 | CuO | 20 |
| AC | $Cu(NO_3)_2/Cr(NO_3)_3 = 1:5$[a] | 350 | $Cr_2O_3$ | 88 |
| AC | $Cu(NO_3)_2/Cr(NO_3)_3 = 5:1$[a] | 350 | CuO | 10 |
| CA | $Cu(NO_3)_2$ | 500 | CuO | <10 |
| CA | $Cr(NO_3)_3$ | 500 | $Cr_2O_3$ | 87 |

[a] Cu/Cr molar ratio

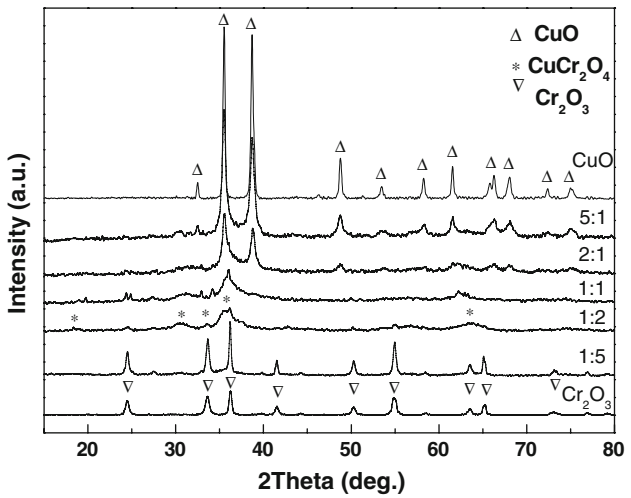


**Fig. 2** XRD patterns of the Cu–Cr catalysts with different Cu/Cr molar ratio prepared by template route and calcined at 500 °C

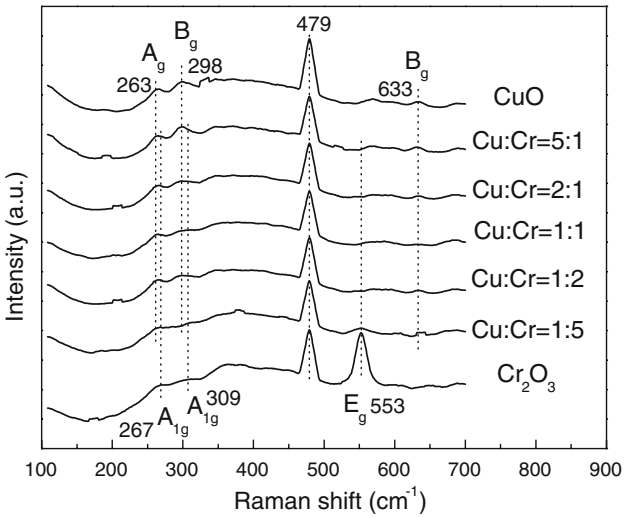


**Fig. 3** Raman spectra of CuO, $Cr_2O_3$, and samples with Cu/Cr molar ratios of 5:1, 2:1, 1:1, 1:2, and 1:5 obtained by carbon template route calcined at 500 °C

calculated using the Scherrer formula. When Cu/Cr molar ratio is 1:1, the obtained sample is called as copper-chromite. From the XRD pattern, broad peaks due to $CuCr_2O_4$ can be observed and no obvious peak can be assigned to CuO, indicating the particle sizes of $CuCr_2O_4$ and CuO are not too big. With the further increase of Cu/Cr molar ratio, the peaks due to CuO become sharp, indicating big particle size of CuO.

Figure 3 shows the Raman spectra of the samples. CuO belongs to the $C_{2h}^6$ space group with two molecules per primitive cell. There are three acoustic modes ($A_u + 2B_u$), six infrared active modes ($3A_u + 3B_u$), and only three Raman active modes ($A_g + 2B_g$) [21–23]. The peak at 263 $cm^{-1}$ in CuO sample can be assigned to the $A_g$ and the peaks at 298 and 633 $cm^{-1}$ to the $B_g$ modes. We note that these wavenumbers are lower than those reported, probably due to size effects [29–34]. When the grain size increases, there was a slight peak shift of about 2 $cm^{-1}$ to higher wavenumbers. For example, the Raman peaks were found at 263, 298 and 633 $cm^{-1}$ in CuO sample, while in the sample with the Cu/Cr molecule ratio of 1:1, the peaks located at 265, 299, and 634 $cm^{-1}$. Chromium oxide belongs to the $D_{3D}^6$ space group with two molecular $Cr_2O_3$ groups per unit cell. Vibrations with symmetry $A_{1g}$ and $E_g$ are Raman active [32]. Only three modes can be observed in Fig. 4. The peaks at 267, 309, and 553 $cm^{-1}$ can be assigned to $A_{1g}$, $A_{1g}$, and $E_g$. With the increase of Cu loading, the peaks shift to higher wavenumbers. For instance, the peaks from $Cr_2O_3$ sample were found at 267, 609, and 553 $cm^{-1}$. However in the sample with the Cu/Cr molecule ratio of 5:1, all the three peaks weakened and

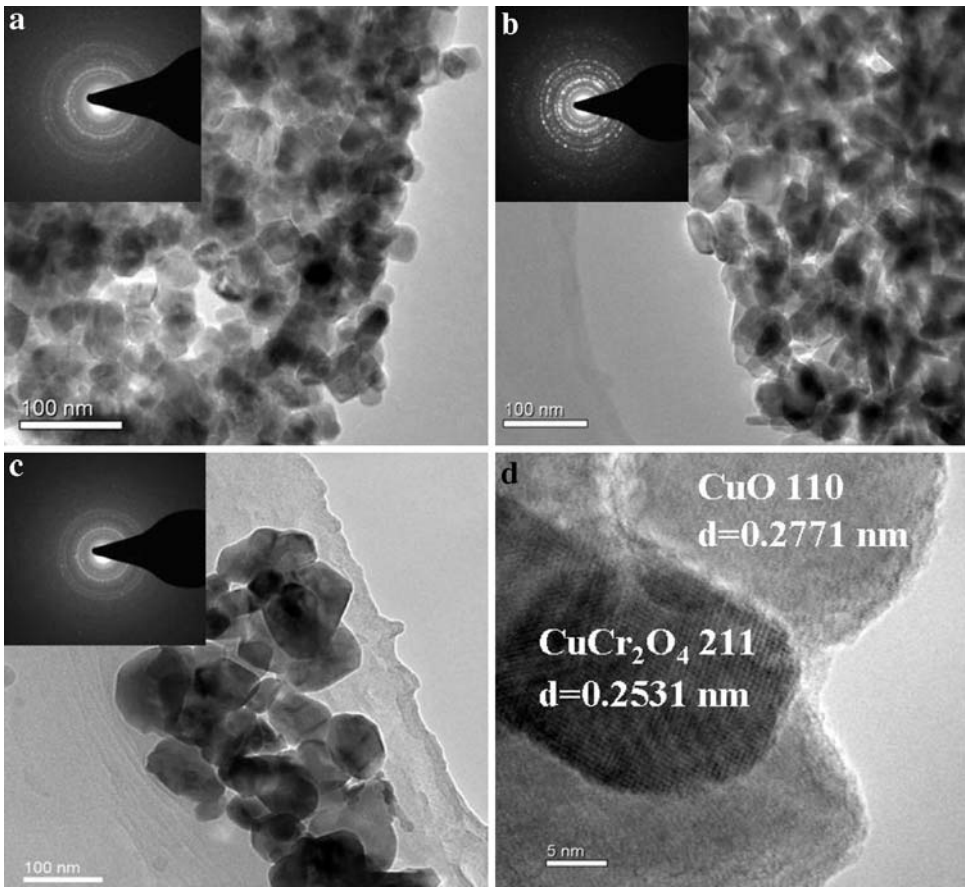


**Fig. 4** TEM and HRTEM images of typical samples obtained at 500 °C by carbon template route **a** Cu/Cr molar ratio = 1:1; **b** $Cr_2O_3$; **c** CuO; **d** HRTEM image of (**a**) sample

only one can be observed which shifted from 553 to 566 $cm^{-1}$. This peak shift may be attributed to size effects [33, 34]. There was one peak without shift can be observed in all the samples at 479 $cm^{-1}$, which was due to the interference. The Raman spectra are consistent with the XRD patterns of the Cu–Cr oxides.

Figure 4 shows the TEM images of CuO, $Cr_2O_3$ and copper-chromite from activated carbon template. As can be seen, the particle size of copper-chromite (Fig. 4a) is about 20 nm, that of $Cr_2O_3$ as sheet-like is about 30 nm (Fig. 4b), and that of spherical CuO particle is about 40 nm. The sizes estimated from TEM are in good agreement with those obtained from XRD. The selected-area electron diffraction (SAED) of copper-chromite, $Cr_2O_3$, and CuO (Fig. 4 inserts) clearly illustrates the crystalline nature of the sample. The samples are spastic structures, not single-crystalline structures, respectively. Figure 5d shows the HRTEM image of copper-chromite sample. The $d$ values measured from the image are 0.2771 and 0.2531 nm of 110 and 211 planes. This can be easily identified to CuO ($d$ = 0.2752 nm, 110 plane) and $CuCr_2O_4$ ($d$ = 0.2548 nm, 211 plane).

$H_2$-TPR profiles of the samples are shown in Fig. 5. In the CuO sample, the only one broad reduction peak from 237 to 390 °C ($T_{max}$ at 330 °C) can be assigned to the reduction of CuO to Cu by $H_2$, while no obvious reduction

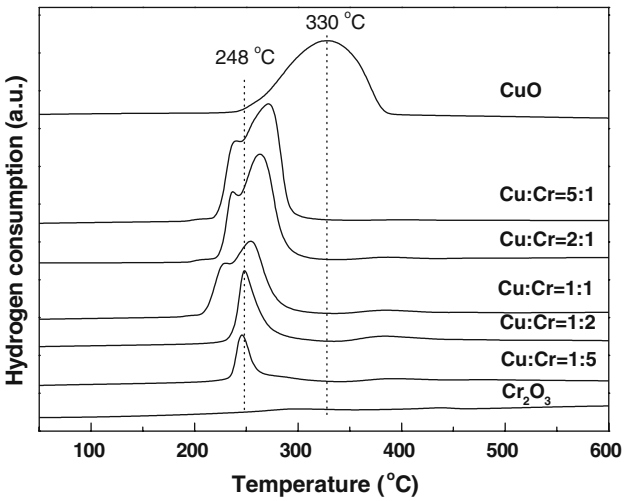


**Fig. 5** $H_2$-TPR profiles of the samples obtained at 500 °C by carbon template route

peak was found in $Cr_2O_3$ sample. For the samples with Cu/Cr molar ratio of 1:2 or 1:5, only one reduction peak at 248 or 245 °C could be detected, which could be assigned to $CuCr_2O_4$ reduction (according to the XRD result). However, for the samples with Cu/Cr ratio of 5:1, 2:1, and 1:1, there are two peaks at about 260 and 230 °C. The peak

with large area (at about 260 °C) could be assigned to reduction of CuO to Cu since the peak areas increase with the increase of Cu/Cr molar ratio, and the small one (at 230 °C) could be assigned to $CuCr_2O_4$ reduction since the peak areas keep constant. There is a shift in the $T_{max}$ of CuO reduction peak from 330 to 253 °C with the decrease of Cu/Cr molar ratio, maybe due to CuO dispersed on $CuCr_2O_4$. With the increase of Cu/Cr molar ratio, the reduction peaks of $CuCr_2O_4$ shift to higher temperature from 225 to 239 °C, probably due to the large particle size. The copper-chromite sample shows the lowest temperatures of CuO reduction ($T_{max}$: 253 °C) and $CuCr_2O_4$ reduction ($T_{max}$: 225 °C), respectively. The results indicate that the interaction between CuO and $CuCr_2O_4$ in copper-chromite is weak and the sample is easily reduced.

Catalytic properties of CuO, $Cr_2O_3$, and Cu–Cr catalysts prepared by a carbon template route were tested for glycerol hydrogenolysis. Before reaction, the obtained samples are reduced with $H_2$ at 340 °C for 2 h. Figure 6 shows the conversion and selectivity of the as-prepared and reduced samples in glycerol hydrogenolysis. The sample with a Cu/Cr molar ratio of 1:2 exhibits the highest conversion of glycerol (51.0%) with a selectivity to 1,2-propanediol of 97.1%. However, the as-prepared sample without reduction only shows the conversion of 4.3% and the selectivity of 98.0%. The result indicates that the reduced copper is the active phase. The reduced sample with a molar ratio of 1:5 is also highly active in glycerol hydrogenolysis, in which the conversion of glycerol is 50.1% and the selectivity is about 96.2%. But the conversion and the selectivity are 4.7 and 97.3%, respectively, if the catalyst is not reduced with $H_2$. For CuO and the samples with a Cu/Cr molar ratio of 5:1, 2:1, and 1:1, the conversions of glycerol are 18.8, 1.4, 1.4, and 2.4%, respectively, and the selectivities to 1,2-propanediol are 98.7, 99.8, 99.2, and 97.8%, respectively. A commercial copper-chromite catalyst without reduction was tested under the same conditions. The conversion of glycerol is about 2.1%, and the selectivity to propanediol is 95.2%. The result is similar to that of copper-chromite from carbon template route. It is obvious that the Cu–Cr catalyst gave high selectivity to 1,2-propanediol and the Cu/Cr molar ratio in the catalyst has an important effect on the conversions of glycerol. The conventional copper-chromite with Cu/Cr molar ratio of 1:1 gave the low activity, while the sample with low Cu/Cr molar ratio (1:2 and 1:5) shows very high activity and selectivity. The conversion of glycerol on the sample with low Cu/Cr molar ratio is close to that in a specially designed multi-clave reactor, while the selectivity to 1,2-propanediol is higher than that reported by Suppes' group [15]. The high activity and selectivity is assigned to the high dispersion of copper on $Cr_2O_3$ and the strong interaction between copper and $Cr_2O_3$ from $CuCr_2O_4$. The findings show that the carbon template route is great potential in synthesis of high surface area Cu–Cr catalyst, and the Cu–Cr catalyst with low Cu/Cr molar ratio is a highly active and selective catalyst for glycerol hydrogenolysis.

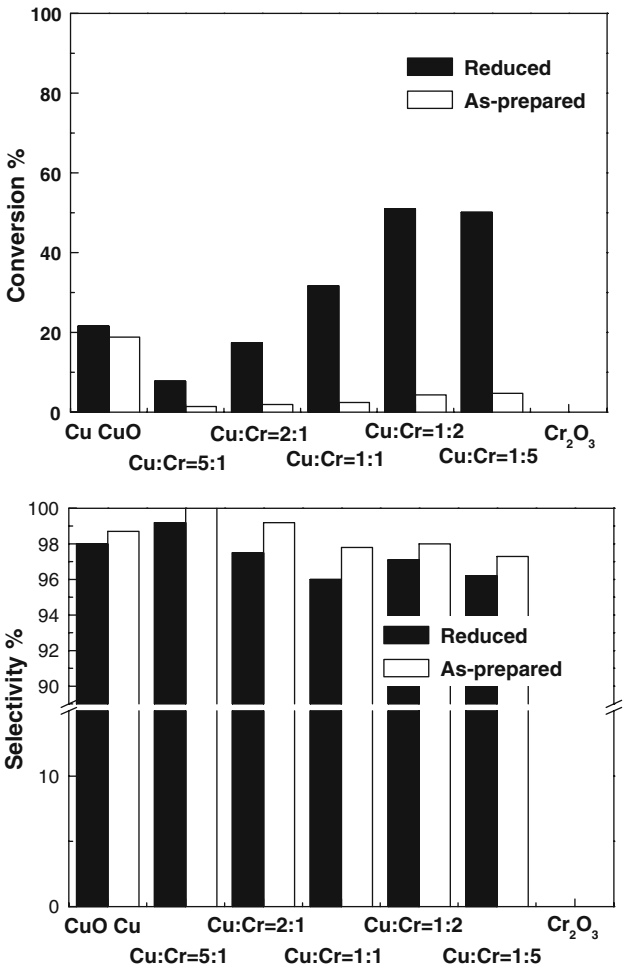


**Fig. 6** Results of glycerol hydrogenolysis over the as-prepared and reduced catalysts (All the reactions were performed using 40% glycerol solution with 5 wt% catalyst in 4.15 MPa $H_2$ at 210 °C for 600 min)

## 4 Conclusion

High surface area Cu–Cr catalysts with different Cu/Cr molar ratio have been synthesized by using carbon materials as templates and copper and/or chromium nitrates as precursors. The surface area of Cu–Cr catalyst can be controlled by carbon template, Cu/Cr molar ratio, and the treatment atmosphere and final temperature. The reduced Cu–Cr catalysts show significant catalytic activity selectivity in glycerol hydrogenolysis, i.e. above 51% conversion of glycerol and above 96% selectivity to 1,2-propanediol. The Cu–Cr catalyst with low Cu/Cr molar

ratio presents high conversion of glycerol, which is different from the conventional copper-chromite. The work also indicates the template route is of great potential in the controlled synthesis of Cu–Cr catalysts with high surface area as a highly active and selective catalyst for glycerol hydrogenolysis.

**Acknowledgment** We gratefully acknowledge the financial support provided by the Program for New Century Excellent Talents in Universities of China (No. NCET-07-0133) and Dalian Science and Technology Foundation (No. 2007J22JH008). The authors thank Prof. Can Li and Prof. Zhaochi Feng for their help in the measurement of Raman spectra.

## References

1. Suppes GJ, Dasari MA, Doskocil EJ, Mankidy PJ, Goff MJ (2004) Appl Catal A 257:213
2. Zhou C, Beltramini JN, Fan Y, Lu G (2008) Chem Soc Rev 37:527
3. Pagliaro M, Ciriminna R, Kimura H, Rossi M, Pina CD (2007) Angew Chem Int Ed 46:4434
4. Ketchie WC, Murayama M, Davis RJ (2005) J Catal 250:264
5. Chaminand J, Djakovitch L, Gallezot P, Marion P, Pinel C, Rosierb C (2004) Green Chem 6:359
6. Wang S, Liu H (2007) Catal Lett 117:62
7. Miyazawa T, Koso S, Kunimori K, Tomishige K (2007) Appl Catal A 329:30
8. Wang K, Hawley MC, DeAthos SJ (2003) Ind Eng Chem Res 42:2913
9. Miyazawa T, Koso S, Kunimori K, Tomishige K (2007) Appl Catal A 318:244
10. Maris EP, Davis RJ (2007) J Catal 249:328
11. Alhanash A, Kozhevnikova EF, Kozhevnikov IV (2008) Catal Lett 120:307
12. Perosa A, Tundo P (2005) Ind Eng Chem Res 44:8535
13. Lahr DG, Shanks BH (2005) J Catal 232:386
14. Miyazawa T, Kusunoki Y, Kunimori K, Tomishige K (2006) J Catal 240:213
15. Dasari MA, Kiatsimkul P, Sutterlin WR, Suppes GJ (2005) Appl Catal A 281:225
16. Adkins H, Connor R, Folkers K (1932) J Am Chem Soc 54:1138
17. Schüth F (2003) Angew Chem Int Ed 42:3604
18. Schwickardi M, Johann T, Schmidt W, Schüth F (2002) Chem Mater 14:3913
19. Liang CH, Qiu JS, Li ZL, Li C (2004) Nanotechnology 15:843
20. Dong A, Ren N, Tang Y, Wang Y, Zhang Y, Hua W, Gao Z (2003) J Am Chem Soc 125:4976
21. Roggenbuck J, Tiemann M (2005) J Am Chem Soc 127:1096
22. Wakayama H, Itahara H, Tatsuda N, Inagaki S, Fukushima Y (2001) Chem Mater 13:2392
23. Kang M, Kim D, Yi SH, Han JU, Yie JE, Kim JM (2004) Catal Today 93–95:695
24. Lin HY, Ma ZQ, Ding L, Qiu JS, Liang CH (2008) Chin J Catal 29:418
25. Kaddouri A, Mazzovvhia C, Tempesti E, Nomen R, Sempere J (1998) J Therm Anal 53:533
26. Prasad R (2005) Mater Lett 59:3945
27. Patron L, Pocol V, Carp O, Modrogan E, Brezeanu M (2001) Mater Res Bull 36:1269
28. Wu D, Fu R, Dresselhaus MS, Dresselhaus G (2006) Carbon 44:675
29. Xu J, Ji W, Shen Z, Tang S, Ye X, Jia D, Xin X (1999) J Solid State Chem 147:516
30. Wang W, Zhuang Y, Li L (2008) Mater Lett 62:1724
31. Xu JF, Ji W, Li WS, Shen ZX, Tang SH, Ye XR, Jia DZ, Xin XQ (1999) J Raman Spectrosc 30:413
32. Chou MH, Liu SB, Huang CY, Wu SY, Cheng C-L (2008) Appl Surf Sci 254:7539
33. Yu T, Zhao X, Shen ZX, Wu YH, Su WH (2004) J Cryst Growth 268:590
34. Zuo J, Xu C, Hou B, Wang C, Xie Y, Qian Y (1996) J Raman Spectrosc 27:921